Finger competition in lifting Hele-Shaw flows with a yield stress fluid

João V. Fontana and José A. Miranda*
Departamento de Física, Universidade Federal de Pernambuco, Recife, PE 50670-901, Brazil
(Received 15 May 2013; published 5 August 2013)

A weakly nonlinear approach is used to investigate interfacial pattern formation in a lifting Hele-Shaw cell containing a yield stress fluid surrounded by a fluid of negligible viscosity. By considering the onset of nonlinear effects and the regime in which viscous effects dominate over yield stress, we study how the system responds to changes in two controlling dimensionless parameters: (i) the geometric aspect ratio (ratio of the initially circular radius of the fluid-fluid interface to the initial Hele-Shaw cell plate spacing), and (ii) a yield stress parameter (relative measure of yield stress to viscous forces). Within this context, we discuss how these key factors influence interface stability and finger competition dynamics during early linear and intermediate stages of pattern evolution.

DOI: 10.1103/PhysRevE.88.023001 PACS number(s): 47.15.gp, 47.54.−r, 47.50.−d, 83.60.La

I. INTRODUCTION

An interesting variation of the traditional radial Saffman-Taylor problem [1] is the study of interfacial instabilities in Hele-Shaw (HS) cells presenting variable gap-spacing. Conventional radial viscous fingering takes place in HS cells having fixed gap widths, where a less viscous fluid is injected into a more viscous one. This induces the emergence of branching fingerlike structures [2–4]. On the other hand, the lifting HS problem occurs when the upper cell plate is lifted while the lower plate remains at rest [5]. In this lifting flow configuration, the inner fluid is viscous (e.g., oil), surrounded by an outer fluid of negligible viscosity (for instance, air). The lifting forces the fluid-fluid interface to move inward. Consequently, the interface becomes unstable, leading to the formation of a distinct class of fingering patterns [6–13].

In contrast to the injection-driven radial viscous flow situation in which finger tip-splitting is the prevalent pattern forming mechanism [1–4], a salient morphological aspect in lifting HS flows is finger competition. Numerical simulations and experiments [5–11] reveal a strong competition (i.e., finger length variability) among the fingers of the invading less viscous fluid, which advance toward the center of the cell. It is also observed that the outermost limit of the interface ceases to shrink, indicating that the competition among the fingering structures of the more viscous fluid is considerably less intense.

The characteristic features of the finger competition dynamics described above are detected in laboratory and numerical experiments when the inner fluid is Newtonian [5–11]. It is true that depending on the nature of the viscous fluid used, different types of interfacial patterns arise [6,12,13]. Nevertheless, inspection of the experimental patterns obtained in Ref. [6] seems to indicate that finger competition phenomena somewhat analogous to those found in Newtonian fluids also occur when the invaded fluid is non-Newtonian. Specifically, in Ref. [6] this happens when the stretched material is a yield stress fluid. Contrary to Newtonian fluids, yield stress fluids [14–16] can support shear stresses without flowing. As long as the stress remains below a certain critical value, they do not flow, but they respond elastically to deformation. Therefore, such materials possess properties of both viscous fluids and elastic solids, behaving like a semisolid substance. Despite the existence of some theoretical works which analyze the development of finger competition in miscible [17] and immiscible [18] lifting HS flows with Newtonian fluids, a corresponding theoretical investigation focusing on the finger competition behavior in yield stress fluids is still lacking.

It has been recently shown [11] that in addition to the material parameters (viscosity, surface tension, etc.) of the fluids involved in lifting HS flows, a purely geometric factor plays an important role in determining pattern shape and evolution. Such a parameter is the aspect ratio, which expresses the ratio of the initially unperturbed circular radius of the fluid-fluid interface to the initial HS plate spacing. Within this context, the aspect ratio measures the cell confinement. The experiments performed in [11] for Newtonian fluids demonstrated that the size and number of growing fingers are significantly sensitive to changes in the aspect ratio. Therefore, one facet of the lifting HS problem that deserves a closer investigation is the influence of the aspect ratio on the finger competition dynamics. This can be done by considering that the inner fluid is either Newtonian or yield stress. A comparative study of the finger competition responses of these fluids during the lifting process is also of interest.

In this work, we carry out the weakly nonlinear analysis of the problem in which a viscous yield stress fluid, surrounded by an inviscid fluid, flows in a lifting HS cell. By exploring the onset of nonlinear effects, we try to gain analytical insight into the dynamic process of finger competition. In particular, we seek to understand how mode-coupling dynamics can describe the influence of both the aspect ratio and the non-Newtonian nature of the distended fluid on the finger competition behavior.

The layout of the rest of the paper is as follows: Section II presents our theoretical weakly nonlinear approach. From a generalized Darcy-like law for yield stress fluids [19], we derive a second-order mode-coupling equation that describes the time evolution of the interfacial amplitudes. This is done by explicitly considering the role played by the inner fluid non-Newtonian nature, as well as the geometric aspect ratio. A discussion on the action of these two elements in regulating finger competition events is presented in Sec. III. Our main results and conclusions are summarized in Sec. IV.

*jme@df.ufpe.br

II. WEAKLY NONLINEAR APPROACH

Finger competition in HS cells is an intrinsically nonlinear effect and cannot be properly addressed by purely linear analysis [1–3]. To elucidate key effects related to finger competition phenomena in lifting HS flow with a yield stress fluid, we employ a weakly nonlinear approach. By doing this, one is able to study both interface stability issues at the early linear regime as well as important morphological aspects at weakly nonlinear, intermediate stages of pattern evolution.

We begin by considering a HS cell of a variable gap width $b(t)\mathcal{C}$ containing a non-Newtonian fluid of viscosity η and yield stress σ_y, surrounded by an inviscid Newtonian fluid (Fig. 1). The surface tension between the fluids is denoted by γ. The upper cell plate can be lifted along the direction perpendicular to the plates (z axis), and the lower plate is held fixed. The initial fluid-fluid interface is circular, having radius $R_0 = R(t=0)$ and initial gap thickness $b_0 = b(t=0)$. By using volume conservation, the time-dependent radius of the unperturbed interface is given by

$$R(t) = R_0\sqrt{\frac{b_0}{b(t)}}. \tag{1}$$

In the lifting HS cell with a yield stress fluid, the flow is governed by two dimensionless equations: a gap-averaged Darcy-like law [19]

$$\nabla P = -\frac{q^2}{b^2}\left[1+\delta\frac{b}{q|\mathbf{v}|}\right]\mathbf{v} \tag{2}$$

and the gap-averaged incompressibility condition [5]

$$\nabla\cdot\mathbf{v} = -\frac{\dot{b}(t)}{b(t)}. \tag{3}$$

In Eq. (2), P is the pressure, $\mathbf{v}$ denotes the fluid velocity, and

$$q = \frac{R_0}{b_0} \tag{4}$$

represents the initial aspect ratio. Moreover,

$$\delta = \frac{\sigma_y b_0}{4\eta|\dot{b}(0)|} \tag{5}$$

is the yield stress parameter that quantifies the ratio between yield stress and viscous forces, where $\dot{b}(t) = db(t)/dt$ is the upper plate velocity along the z axis. We point out that, in Eqs. (2) and (3), in-plane lengths, $b(t)$, and time are rescaled by R_0, b_0, and the characteristic time $T = b_0/|\dot{b}(0)|$, respectively. For the rest of this work, we use the dimensionless version of the equations. As in Ref. [19], we are interested in examining an interface destabilization process, thus we consider the regime where viscous forces prevail over the yield stress and flow is facilitated, which corresponds to $\delta \ll 1$. We refer the reader to our original study [19] for more details on the derivation and validity of our modified Darcy's law model for yield stress fluids [Eq. (2)].

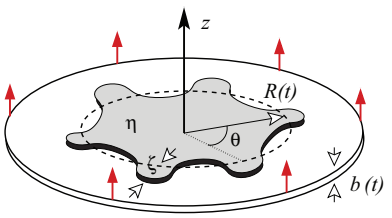

FIG. 1. (Color online) Schematic configuration of the lifting HS cell. The inner fluid (in gray) is a yield fluid of viscosity η, while the outer fluid is Newtonian and has negligible viscosity. The unperturbed time-dependent fluid-fluid interface (dashed curve) is a circle of radius $R = R(t)$. The interface perturbation amplitude is denoted by $\zeta = \zeta(\theta,t)$, and θ is the polar angle. The direction of lifting is along the z axis.

To perform the weakly nonlinear analysis of the system, we consider that the initial circular fluid-fluid interface is slightly perturbed (see Fig. 1), $\Re = R(t) + \zeta(\theta,t)$ ($\zeta/R \ll 1$). The interface perturbation is written in the form of a Fourier expansion $\zeta(\theta,t) = \sum_{n=-\infty}^{+\infty}\zeta_n(t)\exp(in\theta)$, where $\zeta_n(t) = (1/2\pi)\int_0^{2\pi}\zeta(\theta,t)\exp(-in\theta)d\theta$ denotes the complex Fourier mode amplitudes, n is an integer wave number, and θ is the polar angle. The $n=0$ mode is included to keep the area of the perturbed shape independent of the perturbation ζ. Mass conservation imposes that the zeroth mode is written in terms of the other modes as $\zeta_0 = -(1/2R)\sum_{n\neq0}|\zeta_n(t)|^2$. Note that our perturbative analysis keeps terms up to second order in ζ and up to first order in δ.

Taking the divergence of Eq. (2) and using the incompressibility condition (3), the pressure is seen to be anharmonic (nonvanishing Laplacian). Hence, we perform our calculations considering that $\mathbf{v} = \nabla\times\mathbf{A} - \nabla\phi$, where

$$\phi = \frac{\dot{b}r^2}{4b} \tag{6}$$

is a scalar velocity potential [5,18], and

$$\mathbf{A} = \left\{\sum_{n\neq0}A_n\left(\frac{r}{R}\right)^{|n|}\exp(in\theta) + \delta\left[\sum_{n\neq0}\left(\frac{B_n}{r}+\frac{C_n}{r^3}\right)\left(\frac{r}{R}\right)^{|n|}\exp(in\theta)\right]\right\}\hat{\mathbf{z}} \tag{7}$$

is a vector potential. Observe that the vector potential (7) is simply a superposition of a purely Newtonian term ($\propto\delta^0$, coefficients A_n) and a non-Newtonian contribution ($\propto\delta^1$, coefficients B_n),

$$\mathbf{A} = \mathbf{A}_{\mathrm{N}} + \mathbf{A}_{\mathrm{NN}}. \tag{8}$$

The flow described by $\mathbf{A}_{\mathrm{N}}$ is irrotational, while $\mathbf{A}_{\mathrm{NN}}$ has a curl.

Similarly, we express the pressure of the inner fluid as a sum of Newtonian and non-Newtonian pressures, and we propose a general form for their Fourier expansion,

$$P = P_{\mathrm{N}} + P_{\mathrm{NN}}, \tag{9}$$

where

$$P_{\mathrm{N}} = \frac{\dot{b}q^2}{4b^3}r^2 + \sum_{n\neq0}p_n\left(\frac{r}{R}\right)^{|n|}\exp(in\theta) \tag{10}$$

and

$$P_{\mathrm{NN}} = -\frac{\delta q}{b}r + \delta\sum_{n\neq0}\left(\frac{q_n}{r}+\frac{S_n}{r^3}\right)\left(\frac{r}{R}\right)^{|n|}\exp(in\theta). \tag{11}$$

The gradient of the complex pressure field (9) must satisfy the non-Newtonian Darcy's law given by Eq. (2). By inspecting

the r and θ components of (2), and by examining the Newtonian and non-Newtonian components of it, we can express the Fourier coefficients of $P_{\rm N}$, $P_{\rm NN}$, and $\mathbf{A}_{\rm NN}$ in terms of the Fourier coefficients of $\mathbf{A}_{\rm N}$,

$$p_n = -\frac{iq^2\,\mathrm{sgn}(n)}{b^2}A_n, \tag{12}$$

$$q_n = -\frac{iq\beta(n)}{\dot{b}}A_n, \tag{13}$$

$$S_n = \frac{bq}{\dot{b}^2}\sum_{m\neq 0, m\neq n} m(n-m)\mu(n,m)A_m A_{n-m}, \tag{14}$$

$$B_n = \frac{b^2}{q\dot{b}}\alpha(n)A_n, \tag{15}$$

$$C_n = \frac{b^3}{q\dot{b}^2}\sum_{m\neq 0, m\neq n} im(n-m)\nu(n,m)A_m A_{n-m}, \tag{16}$$

where in order to keep the results in a more compact form, we introduced the coefficients

$$\alpha(n) = \frac{2|n|(|n|-1)}{(2|n|-1)}, \tag{17}$$

$$\beta(n) = \frac{2|n|n}{(2|n|-1)}, \tag{18}$$

$$\mu(n,m) = \frac{2}{3(2|n|-3)}[2n\,\mathrm{sgn}(m) + (|n|-3)\mathrm{sgn}[m(n-m)]], \tag{19}$$

and

$$\nu(n,m) = \frac{1}{(|n|-3)}[n\mu(n,m) - 4\,\mathrm{sgn}(m)]. \tag{20}$$

Note that $\mathrm{sgn}(n) = 1$ if $n > 0$ and $\mathrm{sgn}(n) = -1$ if $n < 0$.

Using Eqs. (12)–(16), which are consistent with the solvability condition $\nabla \times \nabla P = \mathbf{0}$ and Darcy's law (2), we can derive the general expression of the vector potential Fourier coefficients in terms of the perturbation amplitudes. To fulfill this goal, consider that the pressure jump condition at the interface can be written as [1,8,9,11]

$$P|_{\Re} = \frac{\Gamma}{q}\kappa_{\parallel}|_{\Re}, \tag{21}$$

where

$$\Gamma = \frac{\gamma}{12\eta|\dot{b}(0)|} \tag{22}$$

is a surface tension parameter and $\kappa_{\parallel}$ is the curvature in the direction parallel to the plates. Equation (21) is the simplest version of the Young-Laplace pressure boundary condition, and it does not include the curvature in the direction perpendicular to the cell plates. Since the depth of the cell varies in lifting Hele-Shaw flows, in principle one could expect the perpendicular curvature to play some role in the dynamics of the system. To the best of our knowledge, the only existing study which discusses the alleged role of the perpendicular curvature in lifting Hele-Shaw flows has been performed by Ben Amar and Bonn [9]. The three-dimensional model presented in Ref. [9] is somewhat involved, and just leads to a modest improved agreement between their experiments and theory. In any case, the validity and accuracy of the simpler condition given in (21) has been substantiated by the excellent agreement between experiments and state-of-the-art numerical simulations performed in Refs. [8,11]. In view of these facts, we choose to use the simpler condition (21).

By expanding Eq. (21) up to second order in ζ and up to first order in δ, one can find the coefficient of the vector potential corresponding to the nth evolution mode, $A_n^{(k)}$, in terms of the kth order in ζ (k = 1, 2) [19,20]. These vector potential coefficients can be introduced into the kinematic boundary condition [1,2],

$$\frac{\partial\Re}{\partial t} = \left[\frac{1}{r}\frac{\partial\Re}{\partial\theta}(-v_\theta) + v_r\right]_{|\Re}, \tag{23}$$

which states that the normal components of each fluid's velocity at the interface equals the velocity of the interface itself. By using Eq. (23) plus Darcy's law (2) and Eq. (21), one can finally find the equation of motion for perturbation amplitudes ζ_n. We present the evolution of the perturbation amplitudes in terms of δ and the kth order in the perturbation amplitude ζ,

$$\dot{\zeta}_n = \dot{\zeta}_n^{(1)} + \dot{\zeta}_n^{(2)}, \tag{24}$$

where

$$\dot{\zeta}_n^{(1)} = \lambda(n)\zeta_n, \tag{25}$$

$$\lambda(n) = \frac{\dot{b}}{2b}(|n|-1) - \frac{\Gamma b^2}{q^3R^3}|n|(n^2-1) + \delta\frac{b|n|}{(2|n|-1)qR}\left[\frac{2\Gamma b^3}{\dot{b}q^3R^3}|n|(n^2-1) - (3|n|-1)\right] \tag{26}$$

is the linear growth rate, and

$$\begin{aligned}\dot{\zeta}_n^{(2)} = &\sum_{m\neq n,0}[F_{\rm N}(n,m) + \delta F_{\rm NN}(n,m)]\,\zeta_m\zeta_{n-m} \\ &+ \sum_{m\neq n,0}[G_{\rm N}(n,m) + \delta G_{\rm NN}(n,m)]\,\dot{\zeta}_m\zeta_{n-m} \\ &+ \delta\sum_{m\neq n,0}H_{\rm NN}(n,m)\,\zeta_m\dot{\zeta}_{n-m} \\ &+ \delta\sum_{m\neq n,0}J_{\rm NN}(n,m)\dot{\zeta}_m\dot{\zeta}_{n-m}.\end{aligned} \tag{27}$$

Equation (24) is the mode-coupling equation of the lifting HS problem with a yield stress fluid. It gives us the time evolution of the perturbation amplitudes ζ_n, accurate to second order, in the weak yield stress limit. Notice that Eq. (24) is conveniently written in terms of three dimensionless quantities: the aspect ratio q [Eq. (4)], the yield stress parameter δ [Eq. (5)], and the surface tension parameter Γ [Eq. (22)]. Since the role of Γ has already been sufficiently discussed in Refs. [5,8,11], we focus on understanding the action of q and δ in determining the stability and shape of the interface.

Despite the complex functional form of the mode-coupling terms in (27), as we will see in Sec. III B, the weakly nonlinear scheme furnishes a fairly simple picture for the important mechanism of finger competition in lifting HS flows. It should be noted that the theoretical results presented in the following sections utilize dimensionless quantities which are extracted from the realistic physical parameters used in the experiments

of Refs. [6,8,11]. In accordance with these experimental studies, we consider that the gap width grows linearly with time, so that the lifting velocity $\dot{b}$ is constant.

III. DISCUSSION

A. Linear regime—Interface stability

We open this section by discussing the physical origin of each term in the linear growth rate expression. Since a positive growth rate $\lambda(n)$ leads to an unstable interface, Eq. (26) tells us that the lifting force contribution appearing as the first term on the right-hand side tends to destabilize the system since $\dot{b} > 0$. On the other hand, the second term proportional to $|n|(n^2 - 1)$ is associated to the surface tension connected to the in-plane curvature, and plays a stabilizing role. It can be noticed that increasingly larger values of q (large confinement) tend to inhibit the stabilizing effect due to surface tension.

The description of the terms proportional to δ in Eq. (26) is as follows: the first contribution is due to the coupling between the surface tension parameter Γ and yield stress, and its net effect is destabilizing. Meanwhile, the second term is uniquely related to yield stress and has a stabilizing role. We have verified that for the typical experimental circumstances of Refs. [6,8,11], this last term is dominant so that the overall linear effect of the term proportional to δ in Eq. (26) is indeed to stabilize the interface. We can also see that strong confinement (high aspect ratio) leads to a less efficient stabilization via yield stress effects.

We continue by briefly discussing some useful information which can be extracted from the linear growth rate (26). The wave number of maximum growth [obtained by setting $d\lambda(n)/dt = 0$] for a Newtonian fluid ($\delta = 0$) can be easily calculated from Eq. (26), yielding

$$n_{\max}^{N} = \sqrt{\frac{1}{3}\left(1 + \frac{q^3 R^3 \dot{b}}{2b^3\Gamma}\right)}. \tag{28}$$

From Eq. (26), one can obtain an explicit solution for the wave number $n_{\max}$ with maximal growth rate for a yield stress fluid ($\delta \neq 0$). Although this expression is rather complex, in the limit $(n_{\max}^{N})^2 \gg n_{\max}^{N} \gg 1$ (which is consistent with experiments [6,8,11]) it simplifies to

$$n_{\max} \approx n_{\max}^{N}\left(1 - \delta\frac{b^2}{\dot{b}qR}\right). \tag{29}$$

One can easily verify that the critical wave number [obtained by setting $\lambda(n) = 0$], which is the maximum wave number for which the growth rate is still positive, is slightly shifted toward lower wave numbers as the yield stress parameter δ is increased.

From the findings presented in this section, it is evident that yield stress effects tend to stabilize the interface in the weak yield stress regime. Since $n_{\max}$ [Eq. (29)] is related to the typical number of fingers formed at the onset of the instability, this means that higher δ would induce the formation of patterns tending to present a decreased number of fingered structures. Additionally, the action of yield stress tends to shorten the band of unstable modes. Conversely, larger q tends to destabilize the system favoring the development of patterns having more fingers.

B. Weakly nonlinear regime—Finger competition

Now the full mode-coupling equation (24) is utilized to study the onset of pattern formation through the coupling of a small number of modes. We proceed by using our weakly nonlinear approach to investigate the interface evolution at second order in ζ. To simplify our discussion, it is convenient to rewrite the complex net perturbation in terms of cosine and sine modes,

$$\zeta(\theta,t) = \zeta_0 + \sum_{n=1}^{\infty}\left[a_n(t)\cos(n\theta) + b_n(t)\sin(n\theta)\right], \tag{30}$$

where $a_n = \zeta_n + \zeta_{-n}$ and $b_n = i\,(\zeta_n - \zeta_{-n})$ are real-valued. Without loss of generality, for the remainder of this work, we choose the phase of the fundamental mode so that $a_n > 0$ and $b_n = 0$. Henceforth, we study the development of interfacial instabilities, and we examine how the yield stress parameter δ and the aspect ratio q affect the finger competition dynamics.

We follow Refs. [3,18] and consider finger length variability as a measure of the competition among fingers. Within our approach, the finger competition mechanism can be described by the influence of a fundamental mode n, assuming n is even, on the growth of its subharmonic mode $n/2$. By using Eqs. (24)–(27), the equations of motion for the subharmonic mode can be written as

$$\dot{a}_{n/2} = \{\lambda(n/2) + \mathcal{C}(n)a_n\}\,a_{n/2}, \tag{31}$$

$$\dot{b}_{n/2} = \{\lambda(n/2) - \mathcal{C}(n)a_n\}\,b_{n/2}, \tag{32}$$

where the finger competition function is given by

$$\mathcal{C}(n) = \frac{1}{2}\left[\mathcal{C}\left(\frac{n}{2}, -\frac{n}{2}\right) + \mathcal{C}\left(\frac{n}{2}, n\right)\right] \tag{33}$$

and

$$\begin{aligned}\mathcal{C}(n,m) = {} & F_{\mathrm{N}}(n,m) + \delta F_{\mathrm{NN}}(n,m) + \lambda(m)[G_{\mathrm{N}}(n,m) \\ & + \delta G_{\mathrm{NN}}(n,m)] + \delta\lambda(n-m)[H_{\mathrm{NN}}(n,m) \\ & + \lambda(m)J_{\mathrm{NN}}(n,m)].\end{aligned} \tag{34}$$

From Eqs. (31) and (32) we verify that a negative $\mathcal{C}(n)$ increases the growth of the sine subharmonic $b_{n/2}$ while inhibiting the growth of its cosine subharmonic $a_{n/2}$. The result is an increased variability among the lengths of fingers of the outer fluid penetrating into the inner one. This effect describes the competition of inward fingers. We stress this is in line with what is observed in numerical simulations [5] and experiments [6–8]. Reversing the sign of $\mathcal{C}(n)$ would exactly reverse these conclusions, such that modes $a_{n/2}$ would be favored over modes $b_{n/2}$. In this case, competition of the outward moving fingers of the inner fluid would have preferential growth.

At this point, we emphasize a few important ideas related to the finger competition mechanism described by Eqs. (31) and (32). The action of the subharmonic mode breaks the n-fold rotational symmetry of the fundamental by alternately increasing and decreasing the length of each of the n fingers. The fact that when $\mathcal{C}(n) < 0$ sine modes $b_{n/2}$ grow and cosine modes $a_{n/2}$ decay does not really mean that finger competition only occurs for inward moving fingers. Actually, finger competition is present for both inward and outward moving

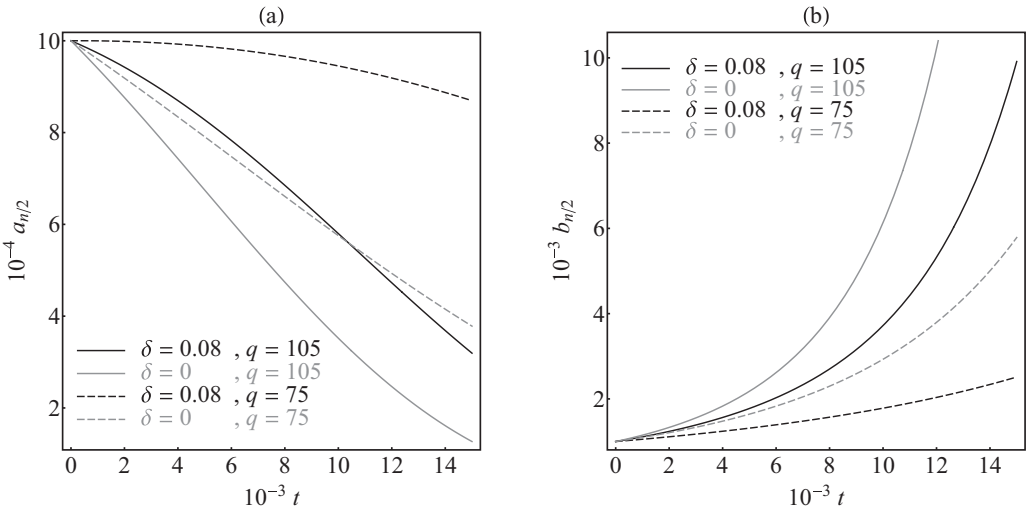

FIG. 2. Time evolution of the (a) cosine ($a_{n/2}$) and (b) sine ($b_{n/2}$) perturbation amplitudes for the subharmonic mode, considering different values of δ and q. Here $a_{n/2}(0) = b_{n/2}(0) = 0.001$, $a_n(0) = 0.01$, $\Gamma = 0.5$, and $t_f = 0.0015$.

fingers. However, while the competition among inward moving fingers is favored, the competition among outward moving fingers is restrained. What our finger competition mechanism determines is the preferred direction for finger growth and finger length variability. So, when $\mathcal{C}(n) < 0$, even though there exists finger competition in both directions (inward and outward), the competition among inward moving fingers is much stronger than the competition among outward moving fingers.

For the typical experimental parameters used in Refs. [6,8,11], we have found that $\mathcal{C}(n) < 0$ indicating a restrained growth of cosine subharmonic modes $a_{n/2}$, accompanied by a simultaneous increased growth of sine subharmonic modes $b_{n/2}$. This general behavior is illustrated in Fig. 2, which depicts the time evolution of the mode amplitudes (a) $a_{n/2}$ and (b) $b_{n/2}$ for different values of the yield stress parameter δ and the aspect ratio q. In Fig. 2, we take the initial amplitudes as $a_{n/2}(0) = b_{n/2}(0) = 0.001$ and $a_n(0) = 0.01$. In addition, $\Gamma = 0.5$, and the final time $t_f = 0.0015$. These parameters are also utilized to plot Figs. 3 and 4.

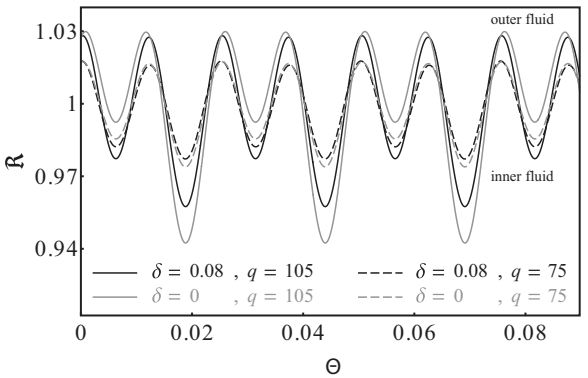

FIG. 3. Snapshot of the fluid-fluid interface position $\Re$ as a function of the polar angle θ at $t = t_f = 0.0015$ for different values of δ and q. This graph uses the same physical parameters utilized in Fig. 2.

In Fig. 2, curves in black (gray) show the amplitudes' time evolution when the inner fluid is yield stress (Newtonian). Moreover, the solid (dashed) curves depict the situation in which the aspect ratio is large (small), given by $q = 105$ ($q = 75$). By inspecting Fig. 2(a), it is clear that the amplitudes of the mode $a_{n/2}$ do tend to decrease as time progresses. Regardless of the value of the aspect ratio q, one observes that the yield stress nature of the inner fluid tends to attenuate such a decrease. It is also evident that stronger attenuation takes place for larger values of q. On the other hand, by examining Fig. 2(b) we notice that the amplitudes of the sine mode $b_{n/2}$ show an increase as time evolves. But, similarly to what has been seen in Fig. 2(a), the growth of $b_{n/2}$ is unfavored for larger (smaller) values of δ (q). Therefore, the main conclusion extracted from Fig. 2 is that finger competition of inward

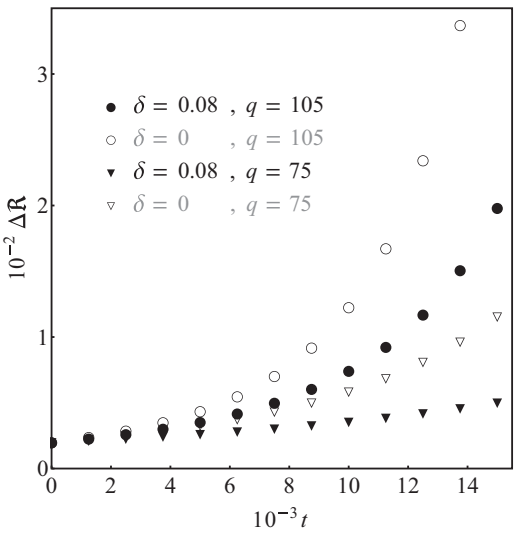

FIG. 4. Difference between the interface positions of the finger tips for consecutive inward moving fingers of the outer fluid $\Delta\Re$ as a function of time for different values of δ and q. This figure uses the same physical parameters utilized in Figs. 2 and 3.

moving fingers is facilitated for stronger confinement (i.e., larger q) and inhibited for higher yield stress effects (larger δ).

To reinforce the conclusions reached from Fig. 2, and to illustrate our finger competition findings in a more pictorial way in Fig. 3, we plot the fluid-fluid interface at final time $t = t_f = 0.0015$ as a function of the polar angle θ. Recall that here we consider the same initial conditions and physical parameters used in Fig. 2. This is done for different values of δ and q. The most noteworthy feature of Fig. 3 is the conspicuous competition between the inward moving fingers of the outer fluid penetrating the inner fluid. It is also clear that the outward moving fingers of the inner fluid do not tend to compete as much. All these more visual verifications are in agreement with the predictions based on the mode-coupling equations (31) and (32), and with the fact that the finger competition function $\mathcal{C}(n)$ is negative. By examining Fig. 3, we can also confirm the fact that the finger competition of inward moving fingers is enhanced for larger values of the aspect ratio and repressed by yield stress effects.

Complementary information about the time evolution of the finger competition behavior in our system can be obtained by analyzing Fig. 4, which plots the difference in finger lengths for consecutive inward moving fingers $\Delta\Re$ as a function of time, for $0 \leqslant t \leqslant t_f$. Note that the quantity $\Delta\Re$ is obtained by calculating the difference between the interface positions of the finger tips $\Re$ for consecutive inward moving fingers of the outer fluid. Finger length variability (i.e., finger competition) does not change much if q and δ are varied at lower times. However, as time advances we can easily verify that finger competition of inward fingers does increase significantly for higher values of q, and tends to be diminished by the action of yield stress effects.

IV. CONCLUSION

There are several experimental and theoretical studies on the lifting flow problem in the confined geometry of a variable-gap HS cell. Most of these investigations focus on understanding purely linear, early time dynamic stages of the problem, or its advanced time, fully nonlinear dynamics. Researchers consider that an inner fluid (which can be Newtonian or non-Newtonian) is surrounded by another fluid of much smaller viscosity. Under lifting flow circumstances, the fluid-fluid interface deforms, producing a variety of complex interfacial patterns. On the theoretical side, the study of such complicated patterns is usually performed by analytical linear stability analyses, or by sophisticated numerical simulations.

In this work, we used an alternative theoretical tool [3] that enables one to get analytic insight into intermediate, weakly nonlinear stages of the lifting HS cell problem. To do that, we employed a perturbative mode-coupling approach which is valid at the onset of nonlinearities, and allows analytic access not only to linear stability issues, but also to key nonlinear aspects of the interface morphology. This has been done by assuming that the inner fluid is a yield stress fluid. By using a generalized Darcy-like law for yield stress fluids [19], and considering the limit in which viscosity effects prevail over yield stress, we derived a nonlinear differential equation describing the time evolution of the perturbation amplitudes. This equation has been utilized to describe finger competition phenomena in lifting HS cells in terms of two dimensionless controlling parameters: the geometric aspect ratio q (a measure of the HS cell confinement) and a yield stress parameter δ (relative measure of yield stress to viscous forces). Our results indicate that while $\delta > 0$ tends to restrain finger competition of inward moving fingers of the penetrating outer fluid, larger values of q enhance competition among these fingering structures. These conclusions are in general agreement with existing experimental studies [6,8,11].

ACKNOWLEDGMENTS

We thank CNPq for financial support through the program "Instituto Nacional de Ciência e Tecnologia de Fluidos Complexos (INCT-FCx)" and FACEPE through PRONEM Project No. APQ-1415-1.05/10.

APPENDIX: EXPRESSIONS FOR THE SECOND-ORDER TERMS

This Appendix presents the expressions for the second-order Newtonian (N) and non-Newtonian (NN) mode-coupling coefficients which appear in Eq. (27),

$$F_{\mathrm{N}}(n,m) = \frac{\dot{b}}{2bR}\left(n\,\mathrm{sgn}(m) - \frac{|n|}{2} - 1\right) - \frac{\Gamma b^2}{q^3R^4}|n|\left(1 - \frac{nm}{2} - \frac{3m^2}{2}\right), \tag{A1}$$

$$F_{\mathrm{NN}}(n,m) = \frac{b}{2qR^2}\left\{\frac{f(n,m)}{2} + \left[\frac{1}{2} + \frac{2\Gamma b^3}{\dot{b}q^3R^3}\left(1 - \frac{nm}{2} - \frac{3m^2}{2}\right)\right][n\beta(n) - |n|\alpha(n)] + \left[|n| - 1 - (n-m)\frac{(2|m|-1)}{m}\right]\alpha(m) - \frac{|n|\beta(m)}{m}(|m|-1)\right\}, \tag{A2}$$

$$G_{\mathrm{N}}(n,m) = \frac{1}{R}[|n|\mathrm{sgn}(nm) - |n| - 1], \tag{A3}$$

$$G_{\mathrm{NN}}(n,m) = \frac{b^2}{\dot{b}qR^2}\left\{\frac{f(n,m)}{2} - \frac{|n|\beta(m)}{m}(|m|-1) + \left[|n| - 1 - (n-m)\frac{(2|m|-1)}{m}\right]\alpha(m) + n\beta(n) - |n|\alpha(n)\right\}, \tag{A4}$$

$$H_{\mathrm{NN}}(n,m) = \frac{b^2}{2\dot{b}qR^2}f(n,m), \tag{A5}$$

and

$$J_{\mathrm{NN}}(n,m) = \frac{b^3}{\dot{b}^2qR^2}f(n,m), \tag{A6}$$

where

$$f(n,m) = n\nu(n,m) - |n|\mu(n,m). \tag{A7}$$

[1] G. M. Homsy, Annu. Rev. Fluid Mech. **19**, 271 (1987); K. V. McCloud and J. V. Maher, Phys. Rep. **260**, 139 (1995); J. Casademunt, Chaos **14**, 809 (2004).
[2] L. Paterson, J. Fluid Mech. **113**, 513 (1981).
[3] J. A. Miranda and M. Widom, Physica D **120**, 315 (1998).
[4] S. W. Li, J. S. Lowengrub, J. Fontana, and P. Palffy-Muhoray, Phys. Rev. Lett. **102**, 174501 (2009).
[5] M. J. Shelley, F-R. Tian, and K. Wlodarski, Nonlinearity **10**, 1471 (1997).
[6] D. Derks, A. Lindner, C. Creton, and D. Bonn, J. Appl. Phys. **93**, 1557 (2003).
[7] S. Poivet, F. Nallet, C. Gay, J. Teisseire, and P. Fabre, Eur. Phys. J. E **15**, 97 (2004).
[8] A. Lindner, D. Derks, and M. J. Shelley, Phys. Fluids **17**, 072107 (2005).
[9] M. Ben Amar and D. Bonn, Physica D **209**, 1 (2005).
[10] J. Nase, A. Lindner, and C. Creton, Phys. Rev. Lett. **101**, 074503 (2008).
[11] J. Nase, D. Derks, and A. Lindner, Phys. Fluids **23**, 123101 (2011).
[12] S. Sinha, T. Dutta, and S. Tarafdar, Eur. Phys. J. E **25**, 267 (2008).
[13] Y. O. M. Abdelhaye, M. Chaouche, and H. Van Damme, Appl. Clay Sci. **42**, 163 (2008).
[14] H. A. Barnes, J. Non-Newtonian Fluid Mech. **81**, 133 (1999).
[15] P. Moller, A. Fall, V. Chikkadi, D. Derks, and D. Bonn, Philos. Trans. R. Soc. London, Ser. A **367**, 5139 (2009).
[16] Q. Barral, G. Ovarlez, X. Chateau, J. Boujlel, B. Rabideau, and P. Coussot, Soft Matter **6**, 1343 (2010).
[17] C.-Y. Chen, C.-H. Chen, and J. A. Miranda, Phys. Rev. E **71**, 056304 (2005).
[18] R. M. Oliveira and J. A. Miranda, Phys. Rev. E **73**, 036309 (2006).
[19] J. V. Fontana, S. A. Lira, and J. A. Miranda, Phys. Rev. E **87**, 013016 (2013).
[20] M. Constantin, M. Widom, and J. A. Miranda, Phys. Rev. E **67**, 026313 (2003).